

1 **Distinguishing the effects of Ce nanoparticles from their dissolution products -**
2 **Identification of transcriptomic biomarkers that are specific for ionic Ce in**
3 ***Chlamydomonas reinhardtii***

4 Elise Morel¹, Jessica Dozois¹, Vera I. Slaveykova² and Kevin J. Wilkinson^{1,Ψ}

5 ¹Biophysical Environmental Chemistry Group, University of Montreal, P.O. Box 6128,
6 Succ. Centre-Ville, Montreal, QC

7 ² Environmental Biogeochemistry and Ecotoxicology, Department F.-A. Forel for
8 Environmental and Aquatic Sciences, School of Earth and Environmental Sciences,
9 Faculty of Science, University of Geneva, Uni Carl Vogt, 66, boulevard Carl-Vogt, CH-
10 1211 Genève 4, Switzerland

11

12 ^Ψ kj.wilkinson@umontreal.ca; ORCID: 0000-0002-7182-3624

13 Accepted for publication : *Metallomics*, 2021, 13: mfaa005; DOI:
14 [10.1093/mtomcs/mfaa005](https://doi.org/10.1093/mtomcs/mfaa005)

15

16

17 **Abstract**

18 Cerium (Ce) is a rare earth element that is incorporated in numerous consumer
19 products, either in its cationic form or as engineered nanoparticles (ENPs). Given the
20 propensity of small oxide particles to dissolve, it is unclear if biological responses induced
21 by ENPs will be due to the nanoparticles themselves or rather to their dissolution. This
22 study provides the foundation for the development of transcriptomic biomarkers that are
23 specific for ionic Ce in the freshwater alga, *Chlamydomonas reinhardtii*. exposed either to
24 ionic Ce or to two different types of small Ce ENPs (uncoated, ~10 nm or citrate coated, ~
25 4 nm). Quantitative reverse transcription PCR was used to analyse mRNA levels of four
26 ionic Ce specific genes (*Cre17g.737300*, *MMP6*, *GTR12* and *HSP22E*) that were
27 previously identified by whole transcriptome analysis in addition to two oxidative stress
28 biomarkers (*APX1* and *GPX5*). Expression was characterized for exposures to 0.03 to 3
29 μM Ce, for 60 to 360 minutes and for pH 5.0-8.0. Near linear concentration-response
30 curves were obtained for the ionic Ce and as a function of exposure time. Some variability
31 in the transcriptomic response was observed as a function of pH, which was attributed to
32 the formation of metastable Ce species in solution. Oxidative stress biomarkers analysed
33 at transcriptomic and cellular levels confirmed that different effects were induced for
34 dissolved Ce in comparison to Ce ENPs. The measured expression levels confirmed that
35 changes in Ce speciation and the dissolution of Ce ENPs greatly influence Ce
36 bioavailability.

37 **Introduction**

38 Approximately one consumer product containing engineered nanoparticles (ENPs)
39 is created every day.¹ Their increasing use and diversity of applications (biology, medicine,
40 electronics, optics, cosmetics, textiles, painting, etc.) is largely explained by their unique
41 properties, including a high specific surface area.² Nonetheless, once emitted into
42 environmental matrices, their properties change. In order to decrease their excess surface
43 energy, they will undergo modifications such as agglomeration, adsorption, dissolution or
44 even changes to their crystal structure.³ These modifications will dictate the intrinsic
45 properties of the ENPs and their interfacial reactivities.⁴

46 One of the major difficulties in evaluating the environmental effects of the metal-
47 based ENPs is distinguishing between the effects of dissolution products and the
48 nanoparticles themselves.^{5,6,7} Indeed, many of the metal-based nanoparticles dissolve
49 significantly, especially at environmentally relevant (i.e. low) concentrations.^{8,9} Several
50 authors have postulated that the effects of dissolved Ce to phytoplankton could be
51 neglected with respect to the ENPs.^{10,11,12} Others have shown Ce ENPs to have a lower
52 acute toxicity than ionic Ce.^{13,14} One of the difficulties is that it is technically difficult to
53 quantify ENP dissolution at low particle concentrations.⁹ An alternate strategy would be to
54 distinguish dissolved metal and ENPs at the level of the cell by using biomarkers that are
55 specific to one form or the other of the metal. The use of biomarkers has the added
56 advantage of contributing to our mechanistic understanding of the bioavailability of the
57 toxic species, which can be helpful for assessing environmental risk via an adverse
58 outcome pathways approach.

59 Ideally, a biomarker should give a sensitive and specific molecular signal in
60 response to an environmentally relevant exposure condition.¹⁵ In reality, biomarkers
61 typically respond over a limited concentration range and in some cases, non-linearly with
62 respect to environmental stressors. In addition, environmental media are generally complex
63 and variable, with physicochemical factors such as temperature, pH, water hardness,
64 organic matter content having the potential to influence the activation and intensity of the
65 biomarkers. Therefore, in ecotoxicology, multiple biomarkers are generally used in order
66 to identify effects concentrations.¹⁶ As much as possible, targets should be related to a
67 relevant biological pathway and induction should be related to the dose of the stressor.
68 Nonetheless, it is necessary to keep the number of molecular targets included in the
69 bioassay low enough so that analysis is both affordable and practical.

70 Whole transcriptomic analysis (RNA-Seq) has been used previously to distinguish
71 the effects of different metal oxide nanoparticles,¹⁷ the effects of particle size,¹⁸ the effects
72 of particle coatings¹⁹ and nanoparticles at different stages of their life cycle.²⁰ The present
73 study contributes to the development of a transcriptomic bioassay for ionic Ce, by
74 quantifying mRNA levels of genes that were identified as potential ionic Ce biomarkers in
75 the freshwater eukaryotic green alga *Chlamydomonas reinhardtii*.¹⁹ Quantitative reverse
76 transcription PCR (RT-qPCR) was performed on a number of promising biomarkers as a
77 function of exposure time, dose and pH.²¹ The specificity of the response to ionic Ce was
78 validated by analyzing mRNA levels of selected targets in response to uncoated and citrate
79 stabilized Ce ENPs.

80 **Materials and Methods**

81 *Ce forms of interest*

82 $\text{Ce}(\text{NO}_3)_3$ (ionic Ce) was purchased from Inorganic Ventures (1.0 g L^{-1} ; ICP-MS
83 standard). Uncoated Ce ENPs (nominally 15 - 30 nm) were purchased from Nanostructured
84 & Amorphous Materials as a powder (1406RE). Triammonium citrate stabilized Ce ENPs
85 (nominally 10 nm) were obtained from Byk (Nanobyk®-3810). The measured Ce
86 concentration of the stock suspension of the citrate coated Ce ENPs was $188 \pm 3 \text{ g L}^{-1}$ Ce
87 ENPs. Detailed characterization and preparation of the Ce ENPs can be found in Morel *et*
88 *al.* (2020).¹⁹

89 *Culture and preparation of the microalgae*

90 *C. reinhardtii* is a green microalga that is ubiquitous to fresh waters and is often
91 used for water quality monitoring and studies examining the toxicology of pollutants in
92 natural waters. Details on its specific culture and preparation for experiments involving
93 trace metals can be found in Zhao and Wilkinson (2015).²² In brief, wild type CC-125 (aka
94 137c) from the *Chlamydomonas* resource center was grown at 20°C under conditions of 12
95 h light/12 h dark ($60 \text{ mmol s}^{-1} \text{ m}^{-2}$) using orbital shaking (100 rpm), until algae reached
96 their mid-exponential growth phase in 4×diluted TAP. The cells were then washed 3x with
97 a simplified exposure medium (see below) that contained no Ce. Cell concentrate was
98 added to the exposure solutions in order to obtain $6.5\text{-}10 \times 10^4 \text{ cells mL}^{-1}$ (i.e. 0.15
99 $\text{cm}^2 \cdot \text{mL}^{-1}$). Cell concentrations and cell surface areas were measured using a Multisizer 3
100 particle counter (50 mm aperture; Beckman Coulter).

101 *Algal exposures*

102 Simplified experimental media were used during the exposure so that the chemical
103 speciation of Ce could be precisely controlled. For example, phosphates can precipitate Ce
104 and thus were removed from the exposure media. The absence of phosphates for short time
105 experiments has been shown to not induce any deleterious effects to the microalgae.²³
106 Furthermore, 10^{-5} M $\text{Ca}(\text{NO}_3)_2$ was added to the exposure media in order to help preserve
107 cell wall integrity.²³ Exposures were conducted in triplicate (at least) with independent
108 batches of microalgae and fresh exposure media that were prepared daily. Control
109 treatments were conducted in similar exposure medium as the treated cells but without the
110 addition of any Ce forms.

111 For the time series exposures, cells were exposed to $0.5 \mu\text{M}$ of Ce ($70.1 \mu\text{g Ce L}^{-1}$
112 for the ionic Ce; $86.1 \mu\text{g CeO}_2 \text{ L}^{-1}$ for the Ce ENPs (composed of ~90% CeO_2)¹⁹ in a
113 medium containing 10.0 mM NaHEPES (pH 7.0) and 10^{-5} M $\text{Ca}(\text{NO}_3)_2$. Cells were
114 sampled at 3, 10, 20, 40, 60, 120 and 360 minutes for the determination of Ce biouptake
115 and at 60, 120, 240 and 360 minutes for the analysis of mRNA expression. Cells were
116 pelleted by centrifugation ($2000\times g$, 2 min., 4°C) from 200 mL of the exposure solution.
117 Cell pellets were then resuspended in 1 mL of nuclease-free water before being transferred
118 into 1.5 mL microtubes, where they were again separated ($2000\times g$, 1 min., 4°C), prior to
119 being frozen on dry ice for 10 min. and stored at -80°C until RNA extraction.

120 For the concentration-response exposures, *C. reinhardtii* was exposed for 2 hours
121 to 0.03, 0.05, 0.3, 0.5 or $3 \mu\text{M}$ Ce (nominal Ce concentrations for both ionic Ce and Ce
122 ENPs) in 10.0 mM NaHEPES (pH 7.0) and 10^{-5} M $\text{Ca}(\text{NO}_3)_2$. For exposures examining
123 the effect of pH, Ce was held constant ($0.5 \mu\text{M}$ Ce) while pH was varied by changing the

124 pH buffer: 10.0 mM NaHEPES (pH 7.0, pH 8.0); 10.0 mM NaMES (pH 5.0, pH 6.0). Cell
125 pellets were isolated as described above, for the analysis of mRNA expression.

126 *Ce determinations*

127 Cerium concentrations in the exposure media were quantified by inductively
128 coupled plasma mass spectrometry (ICP-MS, Perkin Elmer Nexion 300X).¹⁹ Dissolved Ce
129 was distinguished from colloidal (ENP) forms using centrifugal ultrafiltration (Amicon
130 ultra-4, 3 kDa molar mass cutoff) by centrifuging 4 mL samples for 20 min. at 3700×g. In
131 order to minimize adsorptive losses to the ultrafiltration membrane, the filtrate was
132 collected and analyzed only after the third centrifugation cycle. Mass balances were
133 determined from Ce concentrations that were measured: (i) in the filtrate; (ii) in the solution
134 remaining above the filter; and (iii) in an acid (69% v/v HNO₃) extraction of the filter. Ce
135 speciation in the exposure media was calculated with Visual Minteq (v3.1) using measured
136 Ce concentrations and a partial pressure of 4.0×10^{-4} atm for CO₂ (to take into account
137 atmospheric contributions of carbonate/bicarbonate).

138 *Ce biouptake*

139 For the analysis of Ce biouptake, 5 mL of 0.1 M EDTA was added to 45 mL of the
140 exposure medium in order to stop biouptake and to simultaneously wash the adsorbed Ce
141 from the cell wall, presumably leaving only internalized Ce.²⁴ After 1 min. in EDTA, the
142 solution was filtered through a nitrocellulose filter (pore size 3.0 μm, Millipore), which
143 was then rinsed three more times with 5 mL of 0.01 M EDTA. A similar filtration protocol
144 was carried out on exposure solutions without added algae, in order to quantify adsorptive
145 losses to the filter. Furthermore, 1 mL of the exposure medium was sampled immediately

146 before and during algal exposition. Algal cells and filters were digested by adding 400 μL
147 of ultrapure HNO_3 (67–70%) and 300 μL of ultrapure H_2O_2 (30%), prior to heating the
148 mixture at 80° C for 5 h (DigiPREP, SCP science).

149 Digests were diluted in MilliQ water and analyzed by ICP-MS. During ICP-MS
150 analysis, a Ce calibration curve was run every 20 samples while blanks and quality control
151 standards were run every 10 samples. Indium was used as an internal standard to correct
152 instrumental drift.

153 *RNA extraction*

154 Frozen cell pellets were thawed and then immediately resuspended in freshly
155 prepared lysis buffer (0.3 M NaCl, 5.0 mM EDTA, 50 mM Tris-HCl (pH 8.0), 2.0% SDS
156 (wt/v), 3.3 U mL^{-1} proteinase K), where they were incubated at 37°C for 15 min. with
157 orbital shaking (300 rpm). Total RNA was isolated by extracting the sample 3x with
158 phenol:chloroform:isoamyl alcohol (25:24:1, pH 6.8), followed by 1x with
159 chloroform:isoamyl alcohol (24:1). At each step, samples were centrifuged (12,000xg, 10
160 min., 4°C) and supernatants were transferred into new tubes. Total RNA was precipitated
161 from the final aqueous phase by isopropanol addition, then washed with 75% ethanol. After
162 a final centrifugation, the pellet was resuspended in 20-30 μL of nuclease-free water. An
163 aliquot (3 μL) was analyzed by automated electrophoresis for RNA quality (RIN number
164 > 7 , $1.8 < \text{ratio } 260/280 < 2.1$, $\text{ratio } 260/230 > 1.8$; Bioanalyzer, Agilent) and spectroscopy
165 (OD260) in order to determine the concentration of RNA (Nanodrop). RNA samples were
166 stored at -80°C until RNA RT-*q*PCR analysis.

167 ***Reverse transcriptase quantitative real-time PCR (RT-qPCR)***

168 Real-time PCR procedures and analysis followed MIQE guidelines.²⁵ Primers and
169 fluorescent probe sets for the Taqman assay were designed using the Roche Universal
170 Probe Library website (www.universalprobelibrary.com). Specificity of the probes
171 was verified using the grep function of the Linux exploitation system with
172 primer sequences searched in two annotation files containing either the transcript
173 or the gene sequences of *C. reinhardtii* (genome v5.3 assembly), allowing for exon
174 overlaps. Exon positions and transcript isoforms were determined for each
175 gene using the JGI Comparative Plant Genomics Portal.²⁶ Total extracted RNA was
176 converted into cDNA using the High Capacity cDNA Reverse Transcription Kit (Applied
177 Biosystems). Controls without reverse transcriptase were prepared in order to verify the
178 absence of contaminating DNA. *qPCR* reactions were performed using the Taqman Fast
179 *qPCR* MasterMix (Applied Biosystems) with a 1/5 dilution of reverse transcription
180 products and primer and probe concentrations of 250 nM and 100 nM, respectively, in a
181 final volume of 10 μ L. ‘No template’ controls were also prepared in order to control for
182 contamination. Enzyme activation was conducted for 20 s at 95°C and followed by 40 dual
183 temperature amplification cycles (1 s at 95°C and 20 s at 60°C) using the QuantStudio 7
184 Flex Real-Time PCR Systems (IRIC Genomics Platform). For each primer pair and
185 probe set, amplification efficiency was assessed using a standard curve and validated when
186 >85%.

187 To generate the standard curve, *qPCR* reactions were performed using cDNA from
188 a mix of RNA samples using a serial dilution of 1/5, 1/25, 1/125 and 1/625. Data were
189 analyzed using the QuantStudio Real-Time PCR software (v1.3). Relative mRNA levels

190 were analyzed using the $2^{-\Delta\Delta CT}$ method with the threshold cycle (CT). Non-induced control
191 genes: *RACK1*²⁷ (CT around 20) and *APG6* (CT around 27 and no observable changes in
192 intensity¹⁹) were used for normalization of the *q*PCR data (**Table S1**). Fold changes
193 between 0.5 and 2.0 were attributed to technical and biological variability rather than a
194 treatment effect.

195 ***Reactive oxygen species (ROS) production and oxidative stress***

196 Flow cytometry was employed to follow the oxidative stress and membrane damage
197 in microalgae exposed under similar conditions as described above, except that nominal
198 concentrations were 0, 0.05, 0.1, 0.5, 1 and 5 μ M for the ionic Ce and 0, 0.5, 1 and 10 μ M
199 for the Ce ENPs. Three 1 mL or 0.5 mL aliquots were taken from each of algal suspensions
200 following 30, 90, 210 or 330 min. of exposure. The 1 mL aliquot was directly analyzed
201 using flow cytometry (BD Accuri C6 Plus, BD) equipped with a 488 nm argon excitation
202 laser and a CSampler (Accuri cytometers Inc., Michigan). A flow rate of 35 μ L min⁻¹ was
203 used to measure cell density and biological parameters including: (i) size and granularity
204 of *C. reinhardtii* using either forward laser scattering ($0 \pm 15^\circ$, forward scatter, FSC) or
205 side scattering ($90 \pm 15^\circ$, side scatter, SSC) and (ii) autofluorescence of chlorophyll (> 670
206 nm, FL3). Oxidative stress and membrane damage of the exposed algae were determined
207 following staining with CellROX green and propidium iodide (PI). Two 0.5 mL aliquots
208 were stained with 5 μ M of CellROX green (Life Technologies Europe BV, Zug,
209 Switzerland) or 7 μ M propidium iodide (PI; Sigma – Aldrich, Buchs, Switzerland) in the
210 dark for 30 min. Negative controls ([Ce] = 0 M) were performed for each exposure time
211 and for each type of measurement. Positive controls were prepared from 0.5 mL of an algal
212 aliquot that was: (i) not exposed to Ce; (ii) incubated for 30 min. in the dark with cumene

213 hydroperoxide (1.2 mM) or (iii) placed in warm water ($T^{\circ} > 50^{\circ}\text{C}$) for 30 min., prior to
214 incubation with the fluorescent markers (CellROX, PI). CellROX green stained cells were
215 followed using green fluorescence channel (530 ± 15 nm, FL1) and PI stained cells via the
216 yellow / orange fluorescence channel (585 ± 20 nm, FL2). Analyses were conducted in
217 triplicate with independent batches of algae and exposure media that were prepared on
218 different days.

219 For each acquisition, a threshold of 10,000 events in the gate corresponding to algal
220 cells was selected. Details on the flow cytometry gating strategy can be found in the
221 Supplemental information (**Figure S1** and **Figure S2**), however, it mainly followed
222 procedures described in Cheloni *et al.* (2013, 2014).^{28,29} The proportions of cells that were
223 present in the different gates of interest were retrieved with the CFlow Plus program, in
224 addition to the average values of the different parameters of interest.

225 *Statistical analyses*

226 Statistical analyses were performed in SigmaPlot (v12.0). Data points presented are
227 determined from biological replicates (i.e. independent cultures), while error bars show the
228 standard deviations. A one way analysis of variance (ANOVA) paired with the Holm-Sidak
229 test were used to compare measured fold change to the threshold values (i.e. RT-qPCR) or
230 to compare treated and untreated microalgae (i.e. cytometry data) with significance defined
231 by * for $p < 0.05$, ** for $p < 0.01$ and *** for $p < 0.001$. This method was also applied for all
232 pairwise multiple comparisons with significant differences highlighted by the different
233 letters when $p < 0.05$.

234

235 **Results and Discussion**

236 *Identification of exposure biomarkers for ionic Ce*

237 Based upon RNA-Seq analysis,¹⁹ a number of candidate transcripts were identified
238 as being specific to ionic Ce. Among the 57 transcripts that were shown to be clearly
239 regulated by Ce,¹⁹ 8 were selected based on the magnitude of their regulation by ionic Ce
240 in regards to controls (i.e. the 4 most up-regulated and the 4 most down-regulated). Further
241 filtering based upon the analysis of their raw expression profiles (**Figure S3**) and their
242 functional annotations led to the selection of four transcripts: three that were induced
243 following exposure to ionic Ce (*Cre17.g737300*, *MMP6* and *GTR12*) and a single transcript
244 (*HSP22E*) that was repressed in its presence (**Table 1**). Transcript levels of ROS-induced
245 genes *APXI*³⁰ and *GPX5*³¹ were added in order to test for occurrence of oxidative stress.

246 RNA-Seq results were first validated using RT-*q*PCR assays (**Table SI**), that were
247 conducted on independent samples of cells, which were exposed to similar exposure
248 conditions (i.e. 0.5 μ M Ce in HEPES, pH 7.0, 120 min. exposure). While the direction of
249 regulation (induction or repression) was similar using RNA-Seq and RT-*q*PCR, the
250 magnitude of the regulation (i.e. fold change values) generally differed (**Table 1**).
251 Differences were attributed to both technical and biological variabilities in the experiments.

252 *Ce biouptake and the induced transcriptomic signals as a function of time*

253 Ce biouptake increased over the first two hours of exposure but appeared to
254 stabilize at longer times (**Figure 1**), consistent with prior results with this microalga.³²
255 Given that Ce concentrations in the medium were constant over the entire exposure period
256 (**Figure S4**), the decreased uptake flux (decrease in slope in Fig. 1) was likely due to

257 biological regulation of the uptake (resulting from an increased efflux or decreased influx)
258 as opposed to chemical effects (precipitation of Ce, depletion of Ce in the medium, etc.).

259 The mRNA levels of the four most sensitive biomarkers (**Table 1**) were quantified
260 during an exposure to 0.5 μM Ce over 360 min. (**Figure 2**). Three patterns of mRNA
261 expression were observed: *Cre17.g737300* increased over time to reach a plateau at 240
262 min. (**Figure 2a**); the expression level of *HSP22E* was repressed over time (**Figure 2d**);
263 whereas the expression levels remained fairly stable for *GTR12* and *MMP6*, over the entire
264 exposure period (**Figure 2b, 2c**). For the oxidative stress marker genes, a significant
265 repression of *APXI* was observed at very short exposure times (Holm-Sidak test, $p < 0.01$)
266 but then values returned to control levels by 120 min. (**Figure S5a**). Expression levels of
267 *GPX5* were stable and showed no sign of being regulated by ionic Ce (**Figure S5b**).

268 *Concentration-response relationship*

269 For a 120 min. exposure to ionic Ce, biomarker expression was examined as a
270 function of the measured concentrations of Ce (nominally 0.03 to 3 μM). Increased
271 expression was observed as a function of concentration for all potential biomarker genes,
272 up to 2-3 μM Ce (**Figure 3**). *APXI* appeared to be repressed only for the highest exposure
273 concentration (ionic Ce $\sim 3 \mu\text{M}$) (**Figure S6a**), whereas expression levels of *GPX5* were
274 stable and showed no sign of being regulated by ionic Ce over the entire tested
275 concentration range (**Figure S6b**).

276 The no effects (mRNA) concentration¹⁶ for a 120 min. exposure was between 0.2
277 μM and 0.5 μM Ce for *MMP6* (Holm-Sidak test, $p < 0.05$) and *HSP22E* (Holm-Sidak test,
278 $p < 0.05$) and between 0.5 and 1 μM for *Cre17.g737300* (Holm-Sidak test, $p < 0.001$) and

279 *GTR12* (Holm-Sidak test, $p < 0.05$) (**Figure 3**). As expected, these values are lower than the
280 values required to observe significant biological effects at the cellular level. For example,
281 an EC_{10} of $9.4 \mu\text{M}$ was observed for a 72 hours fluorescence inhibition assay for
282 *Pseudokirchneriella subcapitata*.³³ The predicted “no-effects” concentration (PNEC)
283 estimated for a Ce salt was around $0.4 \mu\text{M}$ for an ecosystem level study by the same
284 authors, which is in good agreement with the transcriptomic results obtained in this study.³³
285 Finally, Collin *et al.* (2014) estimated a PNEC value of 5.8 nM for Ce ENPs (cerium
286 dioxide).¹³

287 *Role of pH on the transcriptomic signal*

288 Transcript levels of the biomarkers were evaluated for pH variations from 5.0 to
289 8.0 for $0.5 \mu\text{M}$ ionic Ce and a 120 min. exposure time. Based upon thermodynamic
290 calculations (Visual Minteq), free Ce in solution will vary from 99.9% to 5.9% of the total
291 Ce in solution, over the pH range of 5.0 to 8.0. Measured Ce concentrations and calculated
292 ionic Ce were fairly constant between pH 5.0 and 7.0 (**Figure 4**), however, metastable
293 colloidal species, not predicted by equilibrium calculations, are thought to form, especially
294 at the higher pH.^{19,32} For example, significant decreases of 20% of the total Ce (Holm-
295 Sidak test, $p < 0.01$) and nearly all of the dissolved Ce (Holm-Sidak test, $p < 0.001$) were
296 observed when increasing the pH from 7.0 to 8.0 (**Figure 4**), suggesting losses by
297 adsorption on the flask walls and/or the formation of sedimenting precipitates at pH 8.0.
298 Indeed, the near absence of dissolved Ce at pH 8.0 broadly agreed with the transcriptomic
299 responses observed for all of the biomarkers, which were not different from control values
300 at pH 8.0 (**Figure 5, Figure S7**).

301

302 *Biomarker responses for the Ce ENPs*

303 Very little or no dissolved Ce could be detected in the ENP suspensions at pH 7.0
304 (**Table 2**), although this fraction did appear to increase at the lower pH for the citrate coated
305 ENPs. In spite of these very low concentrations (and proportions) of dissolved Ce,
306 biouptake was ~10x higher for the ENPs than it was for dissolved Ce (**Figure S8**), for a
307 similar total Ce concentration in the exposure medium. Y intercepts (i.e. t=0) from the
308 biouptake measurements were greater for ENP biouptake experiments than for the ionic
309 cerium, which probably reflected an important adsorption of the Ce ENPs onto the cell
310 surface.

311 In spite of a much greater sorption/biouptake in the presence of ENPs, induction
312 did not differ from control responses for any of the selected biomarkers, either as a function
313 of time (**Figure 6**) or concentration (**Figure 7**), strongly indicating a specificity for
314 dissolved Ce. This result is important as it shows that these biomarkers could be used to
315 distinguish between the effects of the ENPs and the effects of dissolved Ce. It also
316 demonstrates that there is a clear mechanistic difference between the effect of dissolved Ce
317 and that of Ce ENPs. Note that in spite of our efforts, no specific biomarkers for the Ce
318 ENPs were identified to date. *GTR12* did respond to the citrate coated Ce ENPs, but only
319 at the most acidic pH (pH 5.0, Holm-Sidak test, $p < 0.01$) (**Figure S9**). As postulated
320 earlier,¹⁹ some of the transcriptomic effects observed for the citrate coated Ce ENPs may
321 have come from increased citrate in the medium, rather than from a specific ENP effect,
322 however, this result implied that the effects of these Ce ENPs were due to their dissolution
323 products rather than to the ENP themselves. Admittedly, this point would require a more
324 thorough examination of all potential biomarkers (*Chlamydomonas* has 19,526 predicted

325 transcripts).^{34,35} As expected, based upon the weak response for the ENPs, little variation in
326 the transcriptomic response was observed for the oxidative stress biomarkers (**Figure S10**).

327

328 *Validation of the transcriptomic signatures*

329 mRNA levels generally changed in a single direction as a function of both exposure
330 time and Ce concentration, which is an important point when identifying useful
331 biomarkers. Furthermore, the conditions that were employed in this study did not induce
332 important metabolic changes in *C. reinhardtii* (i.e. no changes in the metabolic pathways
333 that responded to Ce). On the other hand, exposures to ionic Ce led to an overexpression
334 of the reactive oxygen species (ROS) and a modification in the membrane permeability of
335 *C. reinhardtii*, when determined by flow cytometry (**Figure 8 a, d**). For example, after a
336 120 min. exposure to 1 μ M ionic Ce, 10% (Holm-Sidak test, $p \leq 0.001$) of the microalgae
337 presented an excess of ROS and while 7% (Holm-Sidak test, $p \leq 0.05$) showed signs of
338 membrane damage. These physiological effects may result from a direct effect of the ionic
339 Ce on oxidative stress related targets such as *APX1*, which was rapidly repressed by ionic
340 Ce (i.e. 60 min.), especially with increasing concentration. Ce can also indirectly produce
341 ROS through enzymatic inhibition via substitution of the metal cofactors. In this
342 perspective, the highly expressed *MMP6* which translate to a protease make sense as the
343 non-functional enzymes must be removed as fast as possible by the cytoplasm. For the
344 short exposure times used here, similar effects were not observed when the microalgae
345 were exposed to Ce ENPs, even at higher concentrations ($> 1 \mu$ M Ce) (**Figure 8 b, c, e, f**).
346 Indeed, ROS generation and membrane damage have really only been reported in *C.*
347 *reinhardtii* for much longer exposure times (> 12 h) and relatively high concentrations of

348 Ce ENPs.³⁶ In contrast to the ionic Ce, the absence of changes in ROS or biomarker
349 induction in the presence of ENP suggests that the two Ce forms act differently, in
350 agreement with our previous results using *C. reinhardtii*.¹⁹ To further confirm the
351 hypothesis that substantial Ce ENPs remain sorbed to the outer cell wall, further
352 experiments using variable extracting agents should be performed.

353 Nonetheless, not all of the Ce biomarkers were affected in the same manner by
354 exposure time, which may have been related to the specific biological pathways within
355 which the investigated genes were involved. For example, in the case of *HSP22E* and
356 *APXI*, both were induced at early exposure times (i.e. maximum of down-regulation was
357 observed at 60 min.) and both encode chloroplast-targeted proteins that are induced during
358 oxidative stress.³⁷ Given that significant modifications to cell size were observed within 60
359 min. following the exposure of *C. reinhardtii* to 1 μM ($p \leq 0.05$) and 5 μM ($p \leq 0.001$) of Ce
360 (**Figure S11a**), the induction of *Cre17g.737300* that was observed as a function of time
361 and concentration may have reflected perturbations in cell turgor at the higher
362 concentrations of ionic Ce. Indeed, while no precise biological function for the protein that
363 is encoded by *Cre17g.737300* has been yet identified in *C. reinhardtii*, high sulfur keratin-
364 associated transmembrane proteins have been reported to be up-regulated in maize during
365 hydric stress.³⁸ The absence of such an effect (at both the transcriptomic and cellular levels)
366 when the microalgae were exposed to environmentally relevant concentrations of Ce ENPs
367 (**Figure S11b,c**) suggests that the regulation of genes related to cellular processes¹⁹ may
368 allow *C. reinhardtii* to adapt well to short-term and low concentration exposures of the
369 ENPs.

370 **Summary and environmental implications**

371 Due to their high specificity and relative linearity with the respect the concentration
372 of ionic Ce (over an environmentally relevant concentration range), four biomarkers
373 (*Cre17.g737300*, *GTR12*, *MMP6* and *HSP22E*) were identified as being specific to
374 dissolved Ce (likely Ce^{3+}) in *C. reinhardtii*. With their different sensitivities, their
375 simultaneous use could be an appropriate strategy for identifying bioavailable Ce to *C.*
376 *reinhardtii* and perhaps other biological species. Indeed, the low concentrations of
377 dissolved Ce that co-occurred in the suspensions of citrate coated Ce ENPs at pH 5.0 were
378 identified based upon the induction of *GTR12*.

379 One caveat should be noted. A much greater variability in mRNA levels was
380 observed when the pH of media varied. This result likely reflected the complexity of Ce
381 speciation, even in simple aqueous media, resulting from the formation of metastable
382 species, which are likely highly charged and likely to sorb to multiple surfaces including
383 cell walls and exposure container walls.

384 Finally, the specificity of this transcriptomic signature will need to be validated in
385 the presence of other rare earth metals since in nature, they are almost always found as
386 metal mixtures.³⁹ The presence of ligands such as phosphate or natural organic matter
387 should also be validated as they are both likely to attenuate the bioavailability of Ce^{40}
388 and/or the metabolism of the microalgae.⁴¹

389 **Acknowledgments**

390 Funding for this work was provided by the Natural Sciences and Engineering
391 Research Council of Canada (NSERC Discovery and Strategic projects grants) and the

392 Fonds de Recherche du Québec - Nature et Technologies (FRQNT). Special thanks go to
393 Raphaëlle Lambert and Pierre Melançon at IRIC genomic platform (University of
394 Montreal) for their advice and support with RT-qPCR analyses and to Yanxia Wu
395 (Concordia University) for sharing her expertise in *C. reinhardtii* RNA extraction.
396 Acknowledgements are also addressed to Giuila Cheloni and Rebecca Beauvais-Flueck
397 (University of Geneva) for their technical support and expert advice during the flow
398 cytometry analysis. Finally, thanks are addressed to the reviewers for their constructive
399 comments of a previous version of this manuscript. The authors declare that there are no
400 conflicts of interest in this work.

401

402 **Bibliography**

- 403 1. Kulacki, K. J.; Cardinale, B. J.; Keller, A. A.; Bier, R.; Dickson, H., How do stream
404 organisms respond to, and influence, the concentration of titanium dioxide nanoparticles?
405 A mesocosm study with algae and herbivores. *Environmental Toxicology and Chemistry*
406 **2012**, *31*, (10), 2414-2422.
- 407 2. Thié, A.; Jong, L. D.; Issartel, J.; Moreau, X.; Saez, G.; Barthé, I. P.; Bestel, I.;
408 Santaella, C.; Achouak, W., Effects of metallic and metal oxide nanoparticles in aquatic
409 and terrestrial food chains. Biomarkers responses in invertebrates and bacteria.
410 *International Journal of Nanotechnology* **2012**, *9*, (3), 181.
- 411 3. Auffan, M.; Rose, J.; Bottero, J.-Y.; Lowry, G. V.; Jolivet, J.-P.; Wiesner, M. R.,
412 Towards a definition of inorganic nanoparticles from an environmental, health and safety
413 perspective. *Nature Nanotechnology* **2009**, *4*, (10), 634.
- 414 4. Auffan, M. Nanoparticules d'oxydes métalliques: relations entre la réactivité de
415 surface et des réponses biologiques. Université Paul Cézanne-Aix-Marseille III, 2007.
- 416 5. Domingos, R. F.; Simon, D. F.; Hauser, C.; Wilkinson, K. J., Bioaccumulation and
417 effects of CdTe/CdS quantum dots on *Chlamydomonas reinhardtii*-nanoparticles or the
418 free ions? *Environmental Science & Technology* **2011**, *45*, (18), 7664-7669.
- 419 6. Leclerc, S.; Wilkinson, K. J., Bioaccumulation of Nanosilver by *Chlamydomonas*
420 *reinhardtii* Nanoparticle or the Free Ion? *Environmental Science & Technology* **2013**,
421 *48*, (1), 358-364.
- 422 7. Merdzan, V.; Domingos, R. F.; Monteiro, C. E.; Hadioui, M.; Wilkinson, K. J., The
423 effects of different coatings on zinc oxide nanoparticles and their influence on dissolution
424 and bioaccumulation by the green alga, *C. reinhardtii*. *Science of the Total Environment*
425 **2014**, *488*, 316-324.
- 426 8. Liu, J.; Hurt, R. H., Ion Release Kinetics and Particle Persistence in Aqueous Nano-
427 Silver Colloids. *Environmental Science & Technology* **2010**, *44*, (6), 2169-2175.
- 428 9. Hadioui, M.; Leclerc, S.; Wilkinson, K. J., Multimethod quantification of Ag⁺
429 release from nanosilver. *Talanta* **2013**, *105*, 15-19.
- 430 10. Booth, A.; Størseth, T.; Altin, D.; Fornara, A.; Ahniyaz, A.; Jungnickel, H.; Laux,
431 P.; Luch, A.; Sørensen, L., Freshwater dispersion stability of PAA-stabilised cerium oxide
432 nanoparticles and toxicity towards *Pseudokirchneriella subcapitata*. *Science of the Total*
433 *Environment* **2015**, *505*, 596-605.
- 434 11. Taylor, N. S.; Merrifield, R.; Williams, T. D.; Chipman, J. K.; Lead, J. R.; Viant,
435 M. R., Molecular toxicity of cerium oxide nanoparticles to the freshwater alga
436 *Chlamydomonas reinhardtii* is associated with supra-environmental exposure
437 concentrations. *Nanotoxicology* **2016**, *10*, (1), 32-41.
- 438 12. Hoecke, K. V.; Quik, J. T.; Mankiewicz-Boczek, J.; Schamphelaere, K. A. D.;
439 Elsaesser, A.; Meeren, P. V. d.; Barnes, C.; McKerr, G.; Howard, C. V.; Meent, D. V. D.,
440 Fate and effects of CeO₂ nanoparticles in aquatic ecotoxicity tests. *Environmental Science*
441 *& Technology* **2009**, *43*, (12), 4537-4546.

- 442 13. Collin, B.; Auffan, M.; Johnson, A. C.; Kaur, I.; Keller, A. A.; Lazareva, A.; Lead,
443 J. R.; Ma, X.; Merrifield, R. C.; Svendsen, C., Environmental release, fate and
444 ecotoxicological effects of manufactured ceria nanomaterials. *Environmental Science:
445 Nano* **2014**, *1*, (6), 533-548.
- 446 14. Yokel, R. A.; Hussain, S.; Garantziotis, S.; Demokritou, P.; Castranova, V.; Cassee,
447 F. R., The yin: an adverse health perspective of nanoceria: uptake, distribution,
448 accumulation, and mechanisms of its toxicity. *Environmental Science: Nano* **2014**, *1*, (5),
449 406-428.
- 450 15. Klaper, R.; Arndt, D.; Bozich, J.; Dominguez, G., Molecular interactions of
451 nanomaterials and organisms: defining biomarkers for toxicity and high-throughput
452 screening using traditional and next-generation sequencing approaches. *Analyst* **2014**, *139*,
453 (5), 882-895.
- 454 16. Hutchins, C.; Simon, D.; Zerges, W.; Wilkinson, K., Transcriptomic signatures in
455 *Chlamydomonas reinhardtii* as Cd biomarkers in metal mixtures. *Aquatic Toxicology* **2010**,
456 *100*, (1), 120-127.
- 457 17. Simon, D. F.; Domingos, R. F.; Hauser, C.; Hutchins, C. M.; Zerges, W.;
458 Wilkinson, K. J., RNA-Seq analysis of the effects of metal nanoparticle exposure on the
459 transcriptome of *Chlamydomonas reinhardtii*. *Applied and Environmental Microbiology*
460 **2013**, AEM. 00998-13.
- 461 18. Lee, T.-L.; Raitano, J. M.; Rennert, O. M.; Chan, S.-W.; Chan, W.-Y., Accessing
462 the genomic effects of naked nanoceria in murine neuronal cells. *Nanomedicine:
463 Nanotechnology, Biology and Medicine* **2012**, *8*, (5), 599-608.
- 464 19. Morel, E.; Jreije, I.; Tetreault, V.; Hauser, C.; Zerges, W.; Wilkinson, K. J.,
465 Biological impacts of Ce nanoparticles with different surface coatings as revealed by RNA-
466 Seq in *Chlamydomonas reinhardtii*. *Nanoimpact* **2020**, 100228.
- 467 20. Fisichella, M.; Berenguer, F.; Steinmetz, G.; Auffan, M.; Rose, J.; Prat, O., Toxicity
468 evaluation of manufactured CeO₂ nanoparticles before and after alteration: combined
469 physicochemical and whole-genome expression analysis in Caco-2 cells. *BMC Genomics*
470 **2014**, *15*, (1), 700.
- 471 21. Ruijter, J. M.; Pfaffl, M. W.; Zhao, S.; Spiess, A. N.; Boggy, G.; Blom, J.; Rutledge,
472 R. G.; Sisti, D.; Lievens, A.; De Preter, K., Evaluation of qPCR curve analysis methods for
473 reliable biomarker discovery: bias, resolution, precision, and implications. *Methods* **2013**,
474 *59*, (1), 32-46.
- 475 22. Zhao, C.-M.; Wilkinson, K. J., Biotic Ligand Model Does Not Predict the
476 Bioavailability of Rare Earth Elements in the Presence of Organic Ligands. *Environmental
477 Science & Technology* **2015**, *49*, (4), 2207-2214.
- 478 23. Kola, H.; Laglera, L. M.; Parthasarathy, N.; Wilkinson, K. J., Cadmium adsorption
479 by *Chlamydomonas reinhardtii* and its interaction with the cell wall proteins.
480 *Environmental Chemistry* **2004**, *1*, (3), 172-179.
- 481 24. Hassler, C. S.; Slaveykova, V. I.; Wilkinson, K. J., Discriminating between intra-
482 and extracellular metals using chemical extractions. *Limnology and Oceanography:
483 Methods* **2004**, *2*, (7), 237-247.

- 484 25. Bustin, S. A.; Benes, V.; Garson, J. A.; Hellemans, J.; Huggett, J.; Kubista, M.;
485 Mueller, R.; Nolan, T.; Pfaffl, M. W.; Shipley, G. L., The MIQE guidelines: minimum
486 information for publication of quantitative real-time PCR experiments. *Clinical Chemistry*
487 **2009**, *55*, (4), 611-622.
- 488 26. Goodstein, D. M.; Shu, S.; Howson, R.; Neupane, R.; Hayes, R. D.; Fazo, J.; Mitros,
489 T.; Dirks, W.; Hellsten, U.; Putnam, N., Phytozome: a comparative platform for green plant
490 genomics. *Nucleic Acids Research* **2011**, *40*, (D1), D1178-D1186.
- 491 27. Castruita, M.; Casero, D.; Karpowicz, S. J.; Kropat, J.; Vieler, A.; Hsieh, S. I.; Yan,
492 W.; Cokus, S.; Loo, J. A.; Benning, C., Systems biology approach in *Chlamydomonas*
493 reveals connections between copper nutrition and multiple metabolic steps. *The Plant Cell*
494 **2011**, *23*, (4), 1273-1292.
- 495 28. Cheloni, G.; Slaveykova, V. I., Optimization of the C11-BODIPY581/591 dye for
496 the determination of lipid oxidation in *Chlamydomonas reinhardtii* by flow cytometry.
497 *Cytometry Part A* **2013**, *83*, (10), 952-961.
- 498 29. Cheloni, G.; Cosio, C.; Slaveykova, V. I., Antagonistic and synergistic effects of
499 light irradiation on the effects of copper on *Chlamydomonas reinhardtii*. *Aquatic*
500 *Toxicology* **2014**, *155*, 275-282.
- 501 30. Wakao, S.; Chin, B. L.; Ledford, H. K.; Dent, R. M.; Casero, D.; Pellegrini, M.;
502 Merchant, S. S.; Niyogi, K. K., Phosphoprotein SAK1 is a regulator of acclimation to
503 singlet oxygen in *Chlamydomonas reinhardtii*. *Elife* **2014**, *3*, e02286.
- 504 31. Fischer, B. B.; Dayer, R.; Schwarzenbach, Y.; Lemaire, S. D.; Behra, R.; Liedtke,
505 A.; Eggen, R. I., Function and regulation of the glutathione peroxidase homologous gene
506 GPXH/GPX5 in *Chlamydomonas reinhardtii*. *Plant Molecular Biology* **2009**, *71*, (6), 569-
507 583.
- 508 32. El-Akl, P.; Smith, S.; Wilkinson, K. J., Linking the chemical speciation of cerium
509 to its bioavailability in water for a freshwater alga. *Environmental Toxicology and*
510 *Chemistry* **2015**, *34*, (8), 1711-1719.
- 511 33. González, V.; Vignati, D. A.; Pons, M.-N.; Montarges-Pelletier, E.; Bojic, C.;
512 Giamberini, L., Lanthanide ecotoxicity: First attempt to measure environmental risk for
513 aquatic organisms. *Environmental Pollution* **2015**, *199*, 139-147.
- 514 34. Merchant, S. S.; Prochnik, S. E.; Vallon, O.; Harris, E. H.; Karpowicz, S. J.;
515 Witman, G. B.; Terry, A.; Salamov, A.; Fritz-Laylin, L. K.; Maréchal-Drouard, L., The
516 *Chlamydomonas* genome reveals the evolution of key animal and plant functions. *Science*
517 **2007**, *318*, (5848), 245-250.
- 518 35. Blaby, I. K.; Blaby-Haas, C. E.; Tourasse, N.; Hom, E. F.; Lopez, D.; Aksoy, M.;
519 Grossman, A.; Umen, J.; Dutcher, S.; Porter, M., The *Chlamydomonas* genome project: a
520 decade on. *Trends In Plant Science* **2014**, *19*, (10), 672-680.
- 521 36. Pulido-Reyes, G.; Briffa, S. M.; Hurtado-Gallego, J.; Yudina, T.; Leganés, F.;
522 Puentes, V.; Valsami-Jones, E.; Rosal, R.; Fernández-Piñas, F., Internalization and
523 toxicological mechanisms of uncoated and PVP-coated cerium oxide nanoparticles in the
524 freshwater alga *Chlamydomonas reinhardtii*. *Environmental Science: Nano* **2019**, *6*, (6),
525 1959-1972.

- 526 37. Schroda, M.; Vallon, O., Chaperones and proteases. In *The Chlamydomonas*
527 *sourcebook*, Elsevier: 2009; pp 671-729.
- 528 38. Yang, L.; Fu, F.-L.; Deng, L.-Q.; Zhou, S.-F.; Yong, T.-M.; Li, W.-C., Cloning and
529 characterization of functional keratin-associated protein 5-4 gene in maize. *African Journal*
530 *of Biotechnology* **2012**, *11*, (29).
- 531 39. Gonzalez, V.; Vignati, D. A.; Leyval, C.; Giamberini, L., Environmental fate and
532 ecotoxicity of lanthanides: are they a uniform group beyond chemistry? *Environment*
533 *International* **2014**, *71*, 148-157.
- 534 40. Dahle, J. T.; Livi, K.; Arai, Y., Effects of pH and phosphate on CeO₂ nanoparticle
535 dissolution. *Chemosphere* **2015**, *119*, 1365-1371.
- 536 41. Moseley, J.; Grossman, A. R., Phosphate metabolism and responses to phosphorus
537 deficiency. In *The Chlamydomonas sourcebook*, Elsevier: 2009; pp 189-215.
- 538 42. Usadel, B.; Poree, F.; Nagel, A.; Lohse, M.; CZEDIK-EYSENBERG, A.; Stitt, M.,
539 A guide to using MapMan to visualize and compare Omics data in plants: a case study in
540 the crop species, Maize. *Plant, Cell & Environment* **2009**, *32*, (9), 1211-1229.
- 541 43. Thimm, O.; Bläsing, O.; Gibon, Y.; Nagel, A.; Meyer, S.; Krüger, P.; Selbig, J.;
542 Müller, L. A.; Rhee, S. Y.; Stitt, M., MAPMAN: a user-driven tool to display genomics
543 data sets onto diagrams of metabolic pathways and other biological processes. *The Plant*
544 *Journal* **2004**, *37*, (6), 914-939.
- 545

546 **Table 1.** Functional information (MapMan ontology^{42, 43} and JGI Comparative Plant
547 Genomics Portal (Phytozome)²⁶) and fold change in mRNA levels for selected
548 differentially expressed genes (Fold-change > |2.0|) after a 120 min. exposure of *C.*
549 *reinhardtii* to 0.5 μM of ionic Ce (pH 7.0), as determined using RNA-Seq (n=3) and RT-
550 qPCR (n=5 to 7). Four potential ionic Ce exposure biomarkers (*Cre17.g737300*, *MMP6*,
551 *GTR12*, *HSP22E*), 2 oxidative stress biomarkers (*APX1*, *GPX5*) and 2 endogen controls
552 (*APG6*, *RACK1*) were examined.
553

Identification		Functional information		Fold change	
ID	Symbol	Mapman	Phytozome	RNA-Seq	RT-qPCR
<i>Cre17.g737300</i>	-	Not assigned	Ultrahigh sulfur keratin-associated protein	10.7 ± 0.8	5.7 ± 1.0
<i>Cre16.g692200</i>	<i>MMP6</i>	Protein degradation	Metalloproteinase of VMP family	7.3 ± 0.8	13.9 ± 7.0
<i>Cre06.g302050</i>	<i>GTR12</i>	Minor CHO metabolism	1,3-beta-D-glucan synthase	4.9 ± 0.8	17.6 ± 8.2
<i>Cre14.g617450</i>	<i>HSP22E</i>	Protein folding	Heat shock protein 22E	0.3 ± 0.9	0.3 ± 0.1
<i>Cre02.g087700</i>	<i>APX1</i>	Redox	Ascorbate peroxidase	-	0.4 ± 0.2
<i>Cre10.g458450</i>	<i>GPX5</i>	Not assigned	Glutathione peroxidase	-	-
<i>Cre01.g020250</i>	<i>APG6</i>	Protein degradation/Cell organization	Beclin 1	-	-
<i>Cre06.g278222</i>	<i>RACK1</i>	Development	Receptor of activated protein kinase C	-	-

554

555

556 **Table 2.** Total Ce concentrations and percentages of dissolved Ce as a function of pH
 557 after 120 min. exposure of *C. reinhardtii* to 0.5 μM Ce in the form of either citrate coated
 558 Ce ENPs or uncoated Ce ENPs (n= 2 to 6).
 559

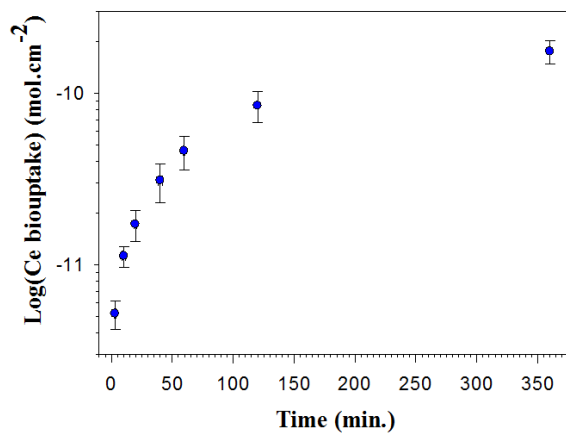
pH	Total Ce concentration (μM)		Dissolved Ce (%)	
	Citrate coated	Uncoated	Citrate coated	Uncoated
5.0	0.28 \pm 0.09	0.35 \pm 0.09	10.0 \pm 8.9	ND
6.0	0.42 \pm 0.07	0.42 \pm 0.04	1.4 \pm 1.7	1.1 \pm 0.4
7.0	0.38 \pm 0.02	0.42 \pm 0.07	0.2 \pm 0.2	ND
8.0	0.28 \pm 0.09	0.39 \pm 0.04	ND	ND

560 ND= Not detected.

561

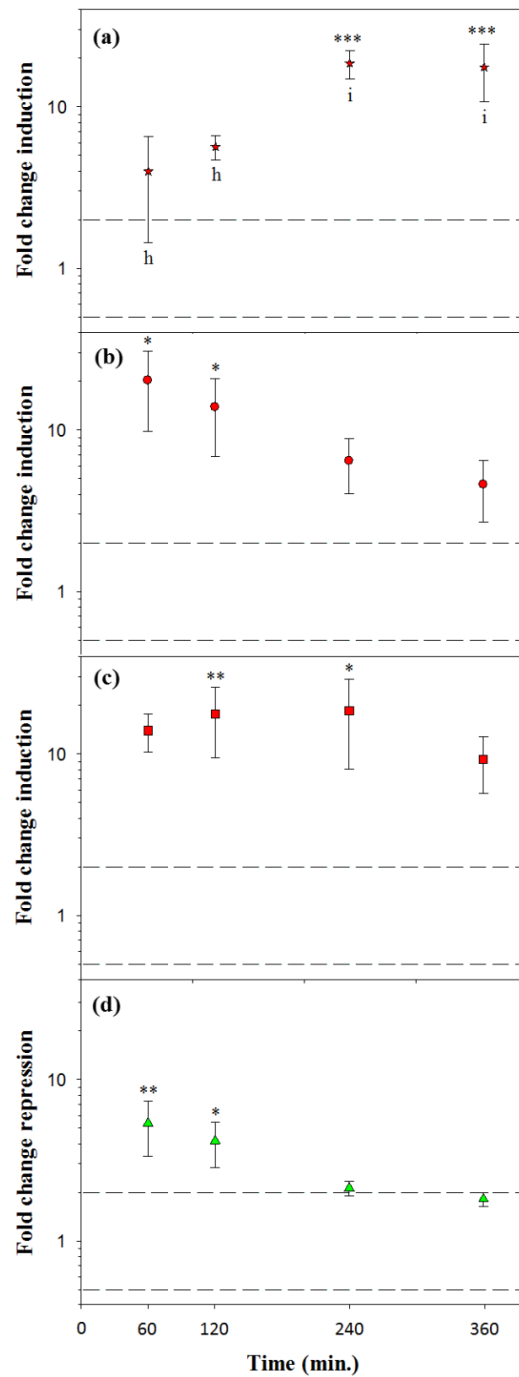
562

563



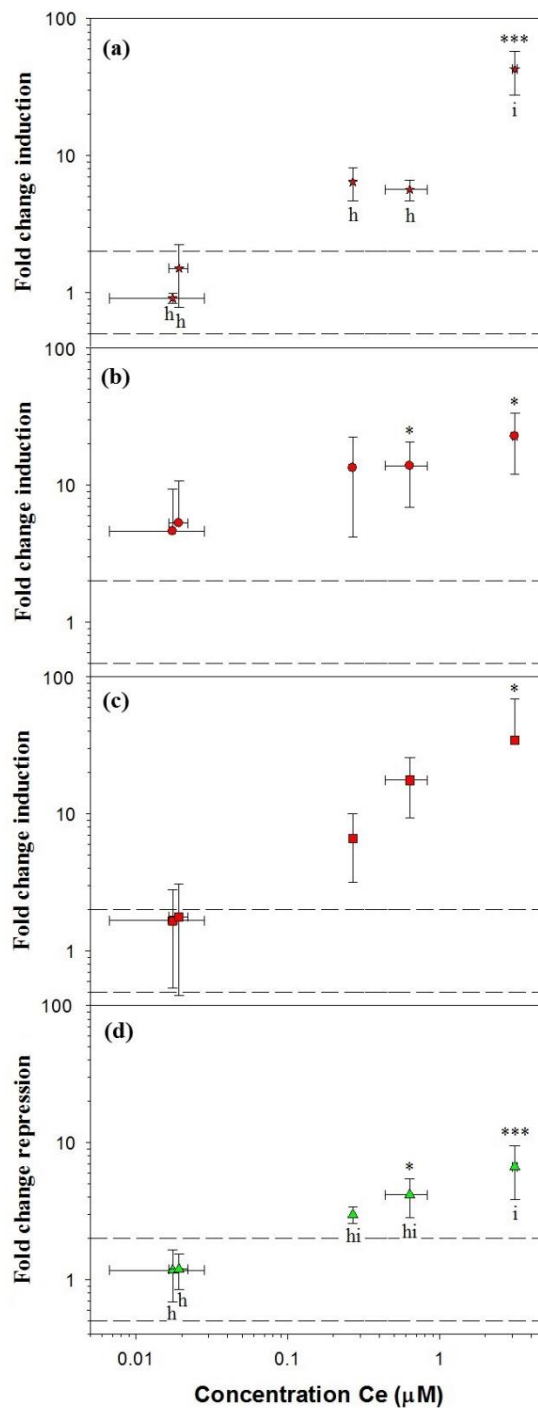
564

565 Figure 1. Ce biouptake by *C. reinhardtii* as a function of exposure time for 0.5 μ M of ionic
566 Ce (n=2 to 3).



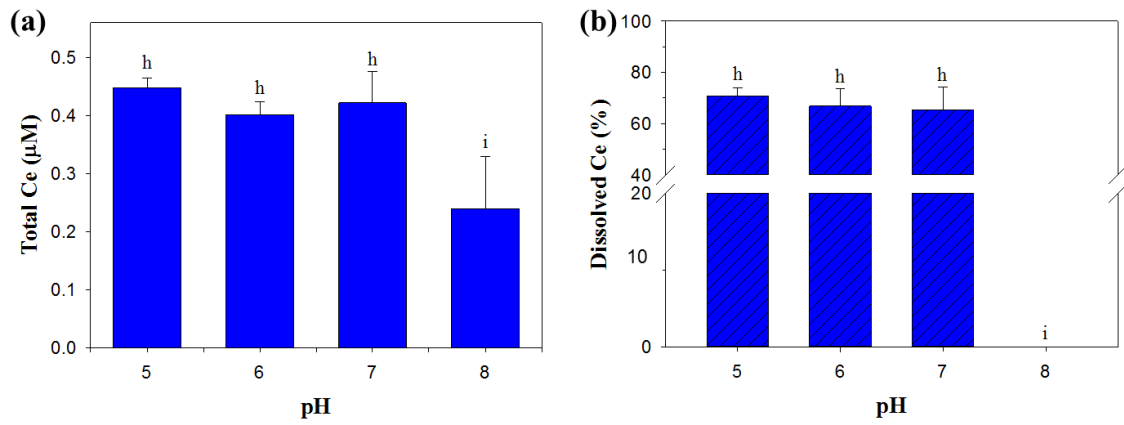
567

568 Figure 2. Fold change induction of (a) *Cre17.g737300*, (b) *MMP6*, (c) *GTR12*, and fold
 569 change repression of (d) *HSP22E* as a function of exposure time for *C. reinhardtii* exposed
 570 to 0.5 μM of ionic Ce. Induced biomarkers are indicated by red points, while repressed
 571 biomarker (=1/fold change induction) is represented by the green points (n=2 to 7). The
 572 dotted lines define the area in which the fold changes of mRNA levels are considered to
 573 occur randomly due to technical and biological variability ($0.5 > \text{fold change} < 2.0$).



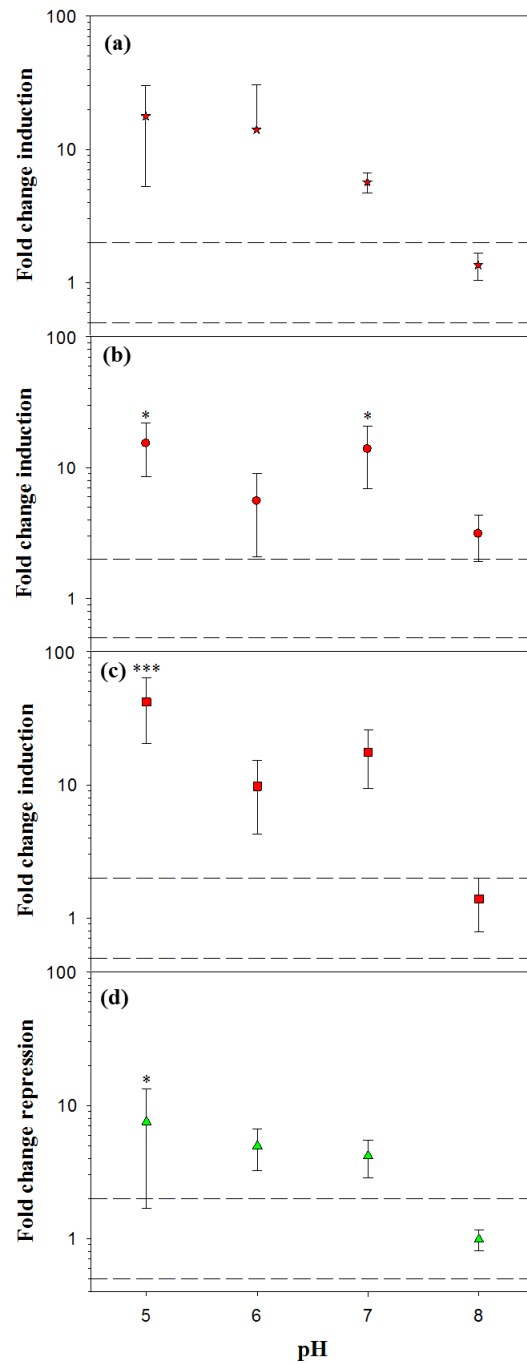
574
 575
 576
 577
 578
 579
 580
 581

Figure 3. Fold change induction of (a) *Cre17.g737300*, (b) *MMP6*, (c) *GTR12*, and fold change repression of (d) *HSP22E* as a function of concentration for a 120 min. exposure of *C. reinhardtii* to ionic Ce (n= 2 to 7). Induced biomarkers are indicated by red points, while the repressed biomarker (=1/fold change induction) is represented by green points. The dotted lines define the area in which fold changes of mRNA levels are considered to occur randomly due to technical and biological variability (0.5>fold change<2.0).



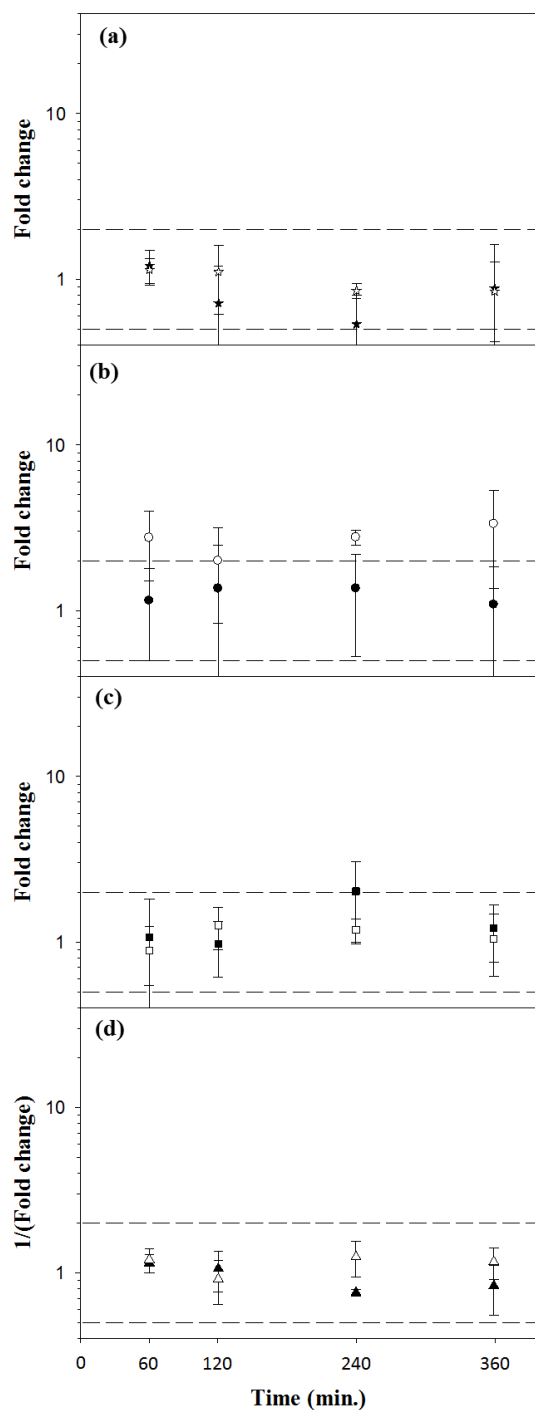
582

583 Figure 4 (a) Total Ce concentration in the exposure media and (b) proportion of dissolved
 584 Ce as a function of pH for a 120 min. exposure of *C. reinhardtii* to 0.5 µM ionic Ce (n= 2
 585 to 6).



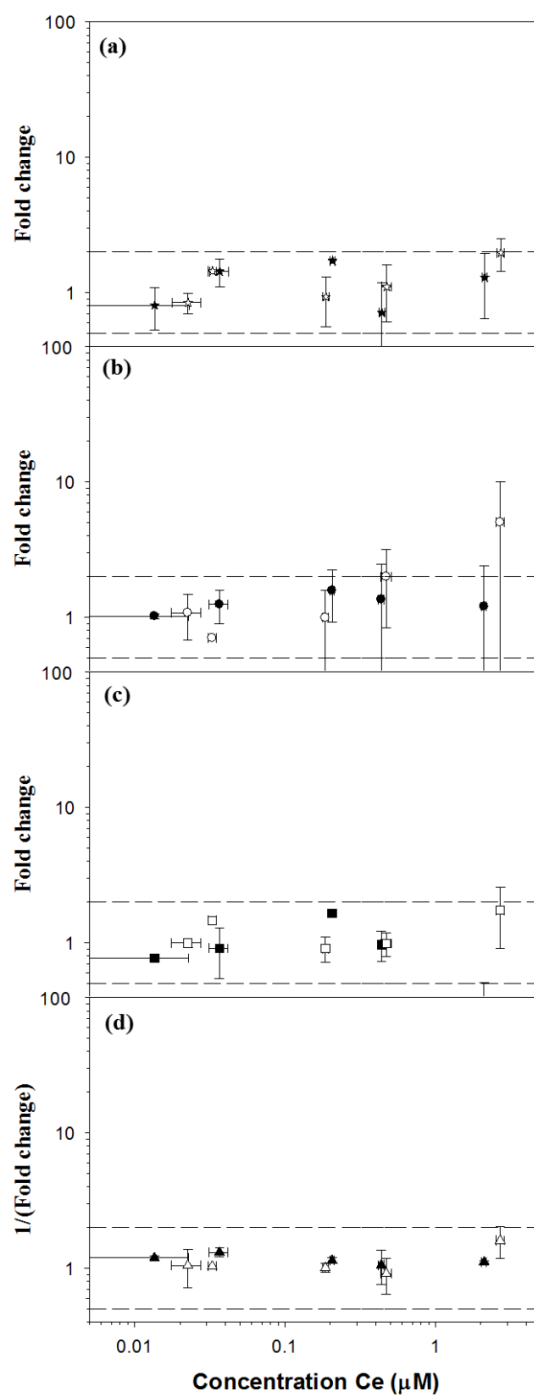
586
 587
 588
 589
 590
 591
 592
 593

Figure 5. Fold change induction of (a) *Cre17.g737300*, (b) *MMP6*, (c) *GTR12*, and fold change repression of (d) *HSP22E* as function of pH for a 120 min. exposure of *C. reinhardtii* to 0.5 μ M of ionic Ce. Induced biomarkers are indicated by red points, while repressed biomarker (=1/fold change induction) is represented by the green points (n= 2 to 7). The dotted lines define the area in which fold changes of mRNA levels are considered to occur randomly due to technical and biological variability ($0.5 > \text{fold change} < 2.0$).



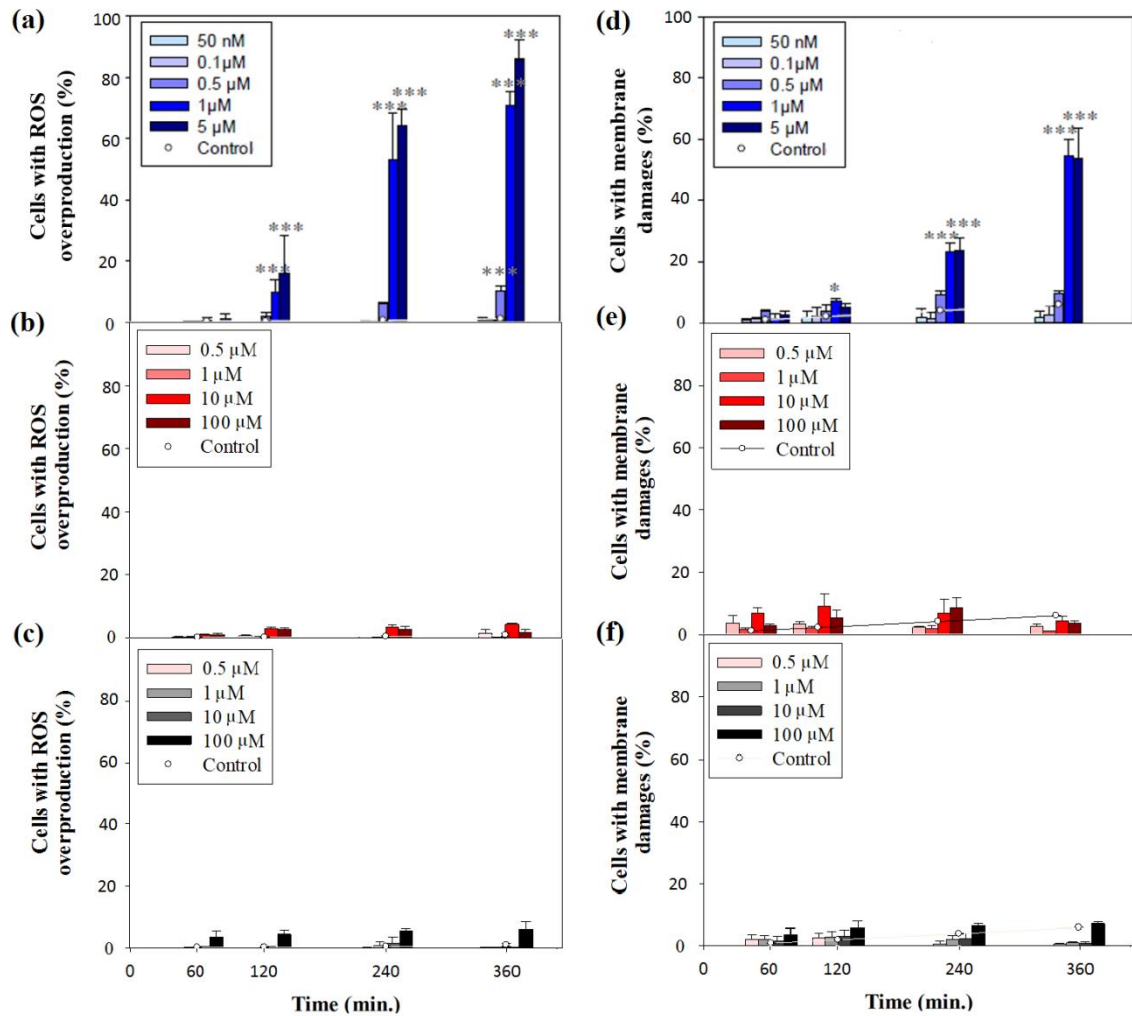
594
 595
 596
 597
 598
 599
 600
 601

Figure 6. Fold change in mRNA levels of (a) *Cre17.g737300*, (b) *MMP6*, (c) *GTR12*, and reciprocal of fold change in mRNA levels of (d) *HSP22E* as a function of exposure time for *C. reinhardtii* exposed to 0.5 μM of total nominal Ce (dissolved and ENP) for citrate coated Ce ENPs (empty symbols) and uncoated Ce ENPs (full symbols) (n=2 to 7). The dotted lines define an area in which the fold change mRNA levels are considered to occur randomly due to technical and biological variability (0.5>fold change<2.0).



602

603 Figure 7. Fold change in mRNA levels of of (a) *Cre17.g737300*, (b) *MMP6*, (c) *GTR12*,
 604 and reciprocal of fold change in mRNA levels of (d) *HSP22E* as a function of the Ce
 605 concentration for a 120 min. exposure of *C. reinhardtii* to citrate coated Ce ENPs (empty
 606 symbols) and uncoated Ce ENPs (full symbols) (n=2 to 7). The dotted lines define the area
 607 in which fold changes of mRNA levels are considered to occur randomly due to technical
 608 and biological variability ($0.5 > \text{fold change} < 2.0$).



609

610 Figure 8. (a, b, c) ROS overproduction and (d, e, f) membrane damage for *C. reinhardtii*
 611 as a function of time and concentration for exposures to (a, d) ionic Ce, (b, e) citrate
 612 coated Ce ENPs and (c, f) uncoated Ce ENPs at pH 7.0 (n=2 to 3).

613